GEOPHYSICAL RESEARCH LETTERS, VOL. ???, XXXX, DOI:10.1029/,

Frequency variability of standing Alfvén waves excited by fast mode resonances in the outer magnetosphere

M. O. Archer,[1,2]

M. D. Hartinger,[3]

B. M. Walsh,[4,5]

F. Plaschke,[6]

V. Angelopoulos,[7]

V. Angelopoulos, Department of Earth, Planetary and Space Sciences, University of California, 603 Charles E. Young Drive, Los Angeles, California, CA 90095-1567, USA. (vassilis@ucla.edu)

M. O. Archer, Space & Atmospheric Physics Group, The Blackett Laboratory, Imperial College London, Prince Consort Road, London, SW7 2AZ, UK. (m.archer10@imperial.ac.uk)

M.D. Hartinger, Electrical and Computer Engineering Department, Virginia Tech, 1185 Perry Street, Blacksburg, VA, 24061, USA. (mdhartin@vt.edu)

F. Plaschke, Space Research Institute, Austrian Academy of Sciences, 8042 Graz, Austria. (Ferdinand.Plaschke@oeaw.ac.at)

B. M. Walsh, Space Sciences Laboratory, University of California, Berkeley, CA, USA. (bwalsh@ssl.berkeley.edu)

[1]Blackett Laboratory, Imperial College

Coupled fast mode resonances (cFMRs) in the outer magnetosphere, between the magnetopause and a turning point, are often invoked to explain observed discrete frequency field line resonances. We quantify their frequency variability, applying cFMR theory to a realistic magnetic field model and magnetospheric density profiles observed over almost half a solar cycle. Our cal-

London, London, SW7 2AZ, UK.

[2]School of Physics & Astronomy, Queen Mary University of London, London E1 4NS

[3]Electrical and Computer Engineering Department, Virginia Tech, Blacksburg, VA, USA.

[4]Department of Mechanical Engineering and Center for Space Physics, Boston University, Boston MA, USA.

[5]Space Sciences Laboratory, University of California, Berkeley, CA, USA.

[6]Space Research Institute, Austrian Academy of Sciences, 8042 Graz, Austria.

[7]Department of Earth, Planetary and Space Sciences, University of California, Los Angeles, CA, USA.

culations show cFMRs are most likely around dawn, since the plasmaspheric plumes and extended plasmaspheres often found at noon and dusk can preclude their occurrence. The relative spread (median absolute deviation divided by the median) in eigenfrequencies is estimated to be 28%, 72% and 55% at dawn, noon and dusk respectively, with the latter two chiefly due to density. Finally, at dawn we show that the observed bimodal density distribution results in bimodal cFMR frequencies, whereby the secondary peaks are consistent with the so-called "CMS" frequencies that have previously been attributed to cFMRs.

1. Introduction

Ultralow frequency (ULF) waves play a number of key roles within the magnetosphere such as the transport, acceleration and loss of electrons in the radiation belts [e.g. the review of *Elkington*, 2006]. One of the earliest known ULF wave modes were field line resonances (FLRs), standing Alfvén waves on field lines fixed at their ionospheric ends [*Southwood*, 1974]. At the resonant field line, position x_r (x, y, z correspond to the radial, azimuthal and field-aligned co-ordinates respectively throughout), they satisfy

$$\left[\frac{\omega}{v_A\left(x_r\right)}\right]^2 - k_z^2 = 0 \tag{1}$$

for angular frequency ω, wavevector component k_z, and local Alfvén speed $v_A = B/\sqrt{\mu_0\rho}$ depending on both magnetic field strength B and plasma mass density ρ. The quantised frequencies of FLRs are often estimated using WKB calculations applied to models i.e.

$$\omega_l\left(x_r\right) = \pi l \left[\int \frac{dz}{v_A}\right]^{-1} \tag{2}$$

where $l \in \mathbb{N}$ denotes the field-aligned mode number (FLR harmonic) and the integral is taken between the field line's footpoints. These show good agreement with observed pulsations, though further sophistications have been developed [*Singer et al.*, 1981; *Wild et al.*, 2005; *Rankin et al.*, 2006; *Kabin et al.*, 2007] which yield small but non-negligible corrections (typically $\sim 20\%$ or less).

Often standing Alfvén waves are excited over a range of L-shells with continuous frequencies [e.g. *Sarris et al.*, 2010]. However, discrete sets of FLRs are also observed, predominantly in the dawn/morning sector with a secondary peak around dusk [*Baker* *et al.*, 2003; *Plaschke et al.*, 2008]. *Samson et al.* [1991, 1992] suggested that a set of quasi-steady FLR frequencies, namely {1.3, 1.9, 2.6–2.7, 3.2–3.4} mHz known as "CMS" frequencies, occur at latitudes ∼70° between midnight–mid-morning. While some statistical studies (of a few hundred events or less) seem to support this hypothesis showing distinct peaks in occurrence distributions [*Fenrich et al.*, 1995; *Chisham and Orr*, 1997; *Mathie et al.*, 1999; *Kokubun*, 2013], larger studies (thousands to tens of thousands of events) show little or no clear peaks [*Ziesolleck and McDiarmid*, 1995; *Baker et al.*, 2003; *Plaschke et al.*, 2008]. The significance of quasi-steady frequencies of discrete FLRs is thus unclear.

A number of potential mechanisms of exciting discrete frequencies of standing Alfvén waves have been proposed including Kelvin-Helmholtz surface waves [*Chen and Hasegawa*, 1974; *Southwood*, 1974], direct driving by solar wind dynamic pressure oscillations [*Stephenson and Walker*, 2002; *Claudepierre et al.*, 2010], and so-called cavity or waveguide modes [*Kivelson. et al.*, 1984; *Kivelson and Southwood*, 1985]. The latter concern radially standing fast magnetosonic waves, trapped between reflecting magnetospheric boundaries and/or turning points. Many types of fast mode resonance (FMR) are known such as plasmaspheric, virtual, tunnelling and trapped modes [see e.g. *Waters et al.*, 2000], but here we focus only on outer-magnetospheric modes which couple to an FLR on the field line where equation 1 is satisfied. These modes propagate between the magnetopause, position x_{mp}, and a turning point inside the magnetosphere, position $x_t \geq x_r$, satisfying (assuming cold plasma)

$$\left[\frac{\omega}{v_A\left(x_t\right)}\right]^2 - k_y^2 - k_z^2 = 0 \tag{3}$$

WKB solutions (which agree within $\sim 3\%$ with full numerical solutions [*Rickard and Wright*, 1995]) involve radially integrating the phase

$$\Phi\left(x_r\right) \equiv \int_{x_t}^{x_{mp}} dx \sqrt{\left[\frac{\omega_l\left(x_r\right)}{v_A\left(x\right)}\right]^2 - k_y^2 - k_z^2} \tag{4}$$

and finding eigenmodes [*Samson et al.*, 1992, 1995]. The turning point introduces a phase shift (weakly dependent on k_y) of $\pi/2$ [*Rickard and Wright*, 1994]. Considering the magnetopause as perfectly reflecting (nodal boundary condition), the eigenmodes correspond to $\Phi\left(x_r\right) = \pi\left(n - \frac{1}{4}\right)$ for radial mode numbers $n \in \mathbb{N}$. Applying this theory, *Samson et al.* [1992] fitted the parameters of an assumed analytical Alfvén speed profile to the CMS frequencies. While this resulted in a reasonable $x_{mp} \sim 15\,\mathrm{R_E}$, some have questioned the field-line lengths used and large densities ($\gtrsim 25\,\mathrm{amu\,cm^{-3}}$) required [*Harrold and Samson*, 1992; *Allan and McDiarmid*, 1993]. *Mann et al.* [1999] later showed that the magnetopause can support anti-nodal boundary conditions, with a quarter wave mode fundamental, which might be able to produce such low frequencies. FMRs with these boundary conditions have been demonstrated in global magnetohydrodynamic simulations [*Claudepierre et al.*, 2009].

The azimuthal wavevector component is often assumed to take the form $k_y = m/x$, where m is the azimuthal mode number [*Waters et al.*, 2000]. m takes discrete values in (closed, axisymmetric) cavity models [*Kivelson. et al.*, 1984], whereas waveguide models consider fast waves propagating towards an open tail whereby m is continuous [*Sam-*

son et al., 1992]. Models of waveguide dispersion show fairly level eigenfrequencies for $|m| \lesssim 3$ and almost constant azimuthal group velocities $\partial\omega/\partial k_y$ for larger $|m|$ which vary only slightly with n [*Wright*, 1994; *Rickard and Wright*, 1994, 1995], hence FMRs show proportionally less dispersion for higher n. While m is a free parameter in most waveguide models, *Mann et al.* [1999] demonstrated a possible m selection mechanism for these modes.

Few unambiguous spacecraft observations of outer-magnetospheric FMRs had been found until fairly recently, largely due to observational difficulties [*Waters et al.*, 2002; *Hartinger et al.*, 2012]. The overall occurrence of FMRs is unclear: *Hartinger et al.* [2013] state a detection rate of $\sim 1\%$ using strict criteria (only cavity modes, biased towards noon) whereas *Hartinger et al.* [2014] provide evidence that FMR-like events occur ~ 37–41% of the time.

Since FLRs transfer energy to radiation belt electrons [*Mann et al.*, 2013] and the ionosphere [*Hartinger et al.*, 2015], predicting when, where and why these occur is important. While direct solar wind driving may account for $\sim 32\%$ of events [*Viall et al.*, 2009], such an assessment for these coupled fast mode resonances (cFMRs) has not yet been possible since observational evidence or lack thereof for cFMRs has often involved searching for the (still heavily disputed) CMS frequencies. However, even cFMR proponents acknowledge that the variability of the magnetosphere should affect these frequencies [*Samson et al.*, 1992; *Walker et al.*, 1992; *Mathie et al.*, 1999]. Models of FMRs typically use either fixed profiles or idealised analytical expressions whereby one parameter is varied [*Allan and McDiarmid*, 1989; *Wright and Rickard*, 1995]. It is not clear how realistic such idealised profiles are and how variable these might be, thus the potential occurrence and variability in frequency/location of outer-magnetospheric cFMRs is unknown. We therefore set out to quantify this variability for the first time.

2. Method

In this study, cFMR theory is applied to dawn, noon and dusk only. Due to the disparity in timescales associated with changes in magnetospheric densities (hours to days [*Khazanov*, 2011]) and magnetic fields (several minutes [*Smit*, 1968]), we treat these quantities independently using observed equatorial density profiles over almost half a solar cycle and a realistic magnetic field model.

Electric Field Instrument (EFI) [*Bonnell et al.*, 2008] and Electrostatic Analyzer (ESA) [*McFadden et al.*, 2008a] measurements from the inner three Time History of Events and Macroscale Interactions during Substorms (THEMIS) [*Angelopoulos*, 2008] probes are used between Feb 2008 – Jun 2013, yielding 5 seasons in each sector. The median magnetic local time (MLT) was calculated for all inbound and outbound magnetosphere crossings (between $3\,\mathrm{R_E}$ and apogee) and only those crossings with sufficient data coverage (>75%) whose median MLT was within 1 h of a target sector were selected. This resulted in 863 (dawn: $6 \pm 1\,\mathrm{h}$ MLT), 809 (noon: $12 \pm 1\,\mathrm{h}$ MLT) and 893 (dusk: $18 \pm 1\,\mathrm{h}$ MLT) crossings. Excluding magnetosheath and solar wind periods using the method of *Lee and Angelopoulos* [2014], electron density profiles n_e were calculated from the spin-averaged spacecraft potential [*McFadden et al.*, 2008b] and binned by radial distance ($0.1\,\mathrm{R_E}$ resolution). A median filter was applied to smooth the profiles but maintain distinct features e.g. the plasmapause. See supporting material for an example. At dawn and dusk since the THEMIS apogees did not extend far enough, a constant extrapolation to the magnetopause was applied [c.f. *Carpenter and Anderson*, 1992]. Changing the extrapolation technique affects our calculations by $\sim 10\%$, but has little effect on their relative variability. To arrive at the plasma mass density, we assume fixed ion compositions in each sector using the results of *Lee and Angelopoulos* [2014] yielding ρ/n_e as 6.8, 2.6 and 4.0 $\mathrm{amu\,cm^{-3}}$ at dawn, noon and dusk respectively. The usual power law form for the density distribution along the field lines was assumed, using exponent $\alpha = 2$ [c.f. *Denton et al.*, 2015]. While these fixed parameters do vary in reality, the effect on cFMR frequency variability is small compared to the density and magnetic field. Figure 1d–f displays histograms (shades of blue) of the density profiles in the three sectors as a function of radial distance. These are largely consistent with previous results e.g. the plasmapause can be seen typically between 4–6 $\mathrm{R_E}$ [*O'Brien and Moldwin*, 2003; *Liu and Liu*, 2014], and higher densities at large radial distances due to either plasmaspheric plumes [*Darrouzet et al.*, 2008; *Walsh et al.*, 2013] or an extended plasmasphere [*Carpenter and Anderson*, 1992; *Tu et al.*, 2007] are more often observed in the noon and dusk sectors.

A model magnetic field is used rather than observed profiles since we require self-consistent FLR frequencies and equatorial Alfvén speeds. Furthermore, the time taken accumulating each density profile is much longer than the variability timescale of the magnetic field. Due to the large variability in equatorial densities [*Sheeley et al.*, 2001; *Takahashi et al.*, 2010, 2014], as a first instance we apply a fixed T96 magnetic field model [*Tsyganenko*, 1995, 1996] (shown in Figure 1a–c) using the median solar wind conditions taken from the OMNI database over the survey period. Combining T96 with the density observations we arrive at Alfvén speed (g–i) and FLR frequency (j–l) profiles, which again are largely consistent with previous observations and models [e.g. *Waters et al.*, 2000; *Archer et al.*, 2013b].

The cFMR theory detailed in equations 1–4 was applied to these profiles for $l = 1$–3 and $|m| = 0$–10 (0.5 spacing). While in idealised box/cylinder models the fast and Alfvén modes are decoupled for $m = 0$ [*Southwood*, 1974], this is not the case in more representative geometries [*Radoski*, 1971]. We use the quantisation condition

$$\Phi\left(x_r\right) = \frac{\pi}{2}\left(n - \frac{1}{2}\right) \tag{5}$$

whereby odd n correspond to modes with an antinode at the magnetopause (e.g. $n = 1$ is a quarter wave mode [*Mann et al.*, 1999; *Claudepierre et al.*, 2009]) whereas even n exhibit nodes [*Samson et al.*, 1992, 1995]. Solving equation 5 yields the resonance locations and eigenfrequencies, denoted $\omega_{l,n}\left(m\right)/2\pi$. The calculations assume plasma properties vary slowly with azimuth compared to the azimuthal propagation of the FMR over a bounce period, found to be $\lesssim$10°, thus are valid in this respect [c.f. *Moore et al.*, 1987].

Since the focus of this study is on variability, we only require that the computed cFMR frequencies are broadly correct since any (small) systematic deviation in absolute values, due to either the WKB approximation or our choice of fixed parameters, will have no effect on the relative variability. Previous studies have indeed shown that the methods used here result in FLR frequencies in good agreement with observations [*Wild et al.*, 2005; *Archer et al.*, 2013a, b]. Throughout this paper the relative spread (or variability) refers to the ratio of median absolute deviation (a robust estimator of scale given by MAD =

$\text{Median}_i (|x_i - \text{Median}_j (x_j)|)$ whereby 50% of the data lie between Median±MAD [*Huber*, 1981]) to the median. This is shown for the density (dotted) and Alfvén speed/FLR frequency (solid) as a function of radial distance in Figure 1m–o.

3. Occurrence

We investigate the possible occurrence of cFMRs (assuming a suitable driver is present at all times) by plotting the fraction of profiles which supported them i.e. a solution to equation 5 existed. This is shown in Figures 2a–c (as a function of n and l for $m = 0$) and 3a–c (as a function of n and m for $l = 1$). It is clear that cFMRs should predominantly occur in the morning sector (e.g. 89% of profiles supported the fundamental mode), being less likely at dusk (65%) and noon (27%). This is in agreement with the occurrence statistics of discrete FLRs [*Baker et al.*, 2003; *Plaschke et al.*, 2008], though of course there are numerous other mechanisms of FLR excitation.

In Figure 1d–l, we plot the median (lines) and interquartile ranges (error bars) for those profiles which did (yellow) and did not (red) support a fundamental cFMR. These reveal, in all sectors though most notably at noon, that cFMR are not supported when the density rises immediately earthward of the magnetopause. In the cFMRs under consideration, fast magnetosonic waves only propagate in regions where $v_A(x) < v_A(x_r)$ [*Waters et al.*, 2000]. Indeed, the profiles which do not support cFMR show decreases in the Alfvén speed with distance from the magnetopause due to the density rising faster than the magnetic field. The size of the cavity is restricted to the vicinity of the magnetopause under these circumstances, making cFMRs impossible. Such density rises may be due to an extended plasmasphere, often observed around noon [*Tu et al.*, 2007; *Archer et al.*, 2013a], or the plasmaspheric plume in the afternoon sector [*Darrouzet et al.*, 2008; *Walsh et al.*, 2013], thereby explaining the possible occurrence of cFMR with local time.

Figures 2a–c and 3a–c show clear trends in possible cFMR occurrence with the mode numbers, being more likely as l increases but less likely as both $|m|$ and n increase. Again, these can be understood in terms of the theory. For a cFMR to be possible, the radial phase integral (equation 4) must become sufficiently large within the outer-magnetospheric cavity (between the magnetopause and plasmapause) such that a radial eigenmode can form (equation 5). Smaller radial mode numbers n require smaller phase integrals, hence are more likely. Increasing the field-aligned mode number l increases the integrand in the phase integral, thereby making a radial eigenmode more likely. Finally, the azimuthal mode number m decreases the integrand serving to push the resonance point Earthward compared to $m = 0$. Since the FLR frequency profiles usually exhibit a peak ahead of the plasmapause, this introduces a maximum possible $|m|$ for which cFMRs are possible, which can be seen when looking at specific examples (not shown).

4. Frequencies

4.1. Density

Here we assess the variability in cFMR frequencies due to density alone. Figure 2 shows the frequencies (d–f) and resonance locations (g–i) as box plots for $m = 0$, where horizontal lines display medians across the profiles, boxes indicate interquartile ranges and whiskers show 95% of the data. The eigenfrequencies are broadly within the expected ranges both theoretically [*Mann et al.*, 1999; *Claudepierre et al.*, 2009] and observationally [*Baker et al.*, 2003; *Plaschke et al.*, 2008; *Hartinger et al.*, 2013], being typically of the order of a few mHz at dawn/dusk and tens of mHz around noon (due to the smaller cavity size and larger Alfvén speeds). As expected, cFMR frequencies increase with both l and n forming an anharmonic series i.e. they are not integer multiples of the fundamental being proportionally more tightly spaced [c.f. *Samson et al.*, 1992]. The resonance locations are at radial distances $\sim$ 4–10 R_E corresponding to magnetic latitudes of $\sim$ 60–75°, within the range of observed discrete FLRs on the ground [*Plaschke et al.*, 2008]. These move towards the magnetopause as l increases, because l increases the phase integrand thus the radial quantisation condition is satisfied earlier; and Earthward for increasing n, due to the larger phase integral required.

While an indication of variability is apparent via the size of the boxes and whiskers in Figure 2, we quantify the relative spreads over all profiles in the frequency (red) and resonance location (blue) for each mode number, shown in panels j–l. It is clear that the variability in resonance location is fairly small in all sectors: $6 \pm 2\%$ (dawn), $14 \pm 3\%$ (noon), $8 \pm 1\%$ (dusk); hence our calculations suggest that the excited FLRs should recur at similar distances/latitudes. Our calculated frequencies, however, display much greater variability, particularly in the noon ($67 \pm 8\%$) and dusk ($49 \pm 2\%$) sectors compared to dawn which exhibits only $18 \pm 1\%$. The level of variability is reflective of the relative spreads in both Alfvén speed and FLR frequency in the outer magnetosphere, as displayed in Figure 1m–o (solid yellow lines for profiles which support cFMR).

Figure 3 indicates how the frequencies and resonance locations are altered as a function of $|m|$ i.e. dispersion. Frequencies and cavity sizes are plotted as the ratio to $m = 0$ results, highlighting changes due to $|m|$ alone by removing the inherent variability at

$m = 0$. As previously noted, increasing $|m|$ pushes the resonance location Earthward (g–i), which serves to increase the cFMR frequency (d–f). The qualitative form of the dispersion and its proportional decrease with n are similar to previous analytical models [*Wright*, 1994; *Rickard and Wright*, 1994, 1995]. Interestingly, there is little spread in the frequency ratios across the profiles ($< 10\%$ at noon and $< 5\%$ at daewn/dusk) indicating that the proportional dispersion is systematic. While m is a free parameter in our cFMR model, *Mann et al.* [1999] demonstrated an m selection method. Given the systematic nature of the dispersion, we therefore do not add a contribution to the overall cFMR frequency variability due to the possible range of m.

4.2. Magnetic Field

So far we have considered cFMR variability due to the density only, however, changes in the magnetic field may also be important. Since the solar wind dynamic pressure P_{dyn} is the most significant source of magnetic field variability, we repeated our calculations over all density profiles changing this input into T96 by plus/minus one median absolute deviation (calculated over the survey period). This self consistently changes the magnetopause location, magnetic field lines and field strengths.

Changing P_{dyn} has a similarly sized effect on cFMR frequencies in all three sectors whereby enhanced P_{dyn} results in higher frequencies, due to a now smaller cavity and higher Alfvén speeds, with the opposite true when decreasing it. This variability due to the magnetic field is $21 \pm 1\%$ (dawn), $24 \pm 5\%$ (noon) and $21 \pm 2\%$ (dusk). Therefore, at dawn the spread in frequency due to changes in the magnetic field is comparable to that of the density, whereas at noon and dusk these effects are small.

Since we treat densities and magnetic fields independently, we combine these sources of variability to arrive at the overall relative spread in cFMR frequencies. These are found to be 28% (dawn), 72% (noon) and 55% (dusk). For comparison, the relative spread in eigenfrequencies of the proposed eigenmode of the subsolar magnetopause is 25% [*Archer and Plaschke*, 2015] i.e. similar to the cFMR frequency variability in the dawn sector.

4.3. Dawn

Given that our calculated cFMRs around dawn can potentially occur most often and exhibit the least amount of variability in both frequency and resonance location, this sector warrants further investigation. Figure 4(top) shows the relationshop between the cFMR frequencies for the first three radial eigenmodes ($l = 1$, $m = -1$) with the reciprocal square root of the outer-magnetospheric density (at apogee). As one might expect, the cFMR frequencies are found to highly correlate to this quantity and thus the Alfvén speed. The density distribution, shown as both a histogram and kernel density estimate (KDE) [*Bowman and Azzalini*, 1997] at the top left, is found to be bimodal. KDEs of the cFMR frequencies (same mode numbers as above) are displayed in bold in the bottom panel revealing similarly bimodal distributions. While the main population corresponds to densities $\sim 0.4\,\mathrm{cm}^{-3}$ and have frequencies $\gtrsim$3 mHz, the secondary population have larger densities $\sim 3\,\mathrm{cm}^{-3}$ and thus lower frequencies. Curiously, the resulting secondary peaks for the $n = 1$–3 cFMR frequencies are similar (within the absolute errors of our calculations) to the first three CMS frequencies, indicated by the grey areas. We find that these secondary peaks in frequency are rather insensitive to the choice of m (lighter colours show KDEs for $-2 \leq m \leq 0$), unlike the higher frequency primary peak. Finally, the resonance locations of these cFMRs (not shown) typically correspond to latitudes ~70°, in agreement with the original *Samson et al.* [1991, 1992] observations.

It had been questioned whether cFMR theory could explain such low frequencies [*Harrold and Samson*, 1992; *Allan and McDiarmid*, 1993], due to the field-line lengths and large densities used by *Samson et al.* [1992]. By allowing for antinodal magnetopause boundary conditions, *Mann et al.* [1999] postulated that mHz FMR eigenfrequencies may be possible. We have shown that these low frequencies may indeed be explained by cFMRs for a small population of observed density profiles applied to a realistic magnetic field model. However, we do not preclude the possibility that other forms of FMR [e.g. *Harrold and Samson*, 1992; *Waters et al.*, 2000] might also explain similar frequency discrete FLRs or that they may be excited via other mechanisms e.g. directly by solar wind pressure oscillations [*Viall et al.*, 2009].

5. Conclusions

Due to observational challenges and conflicting results, it has been unclear how often standing Alfvén waves are excited by coupled fast mode resonances (cFMRs) in the outer magnetosphere (between the magnetopause and a turning point) and what their range of frequencies are. Through the use of a realistic magnetic field model and observed magnetospheric density profiles over almost half a solar cycle, we have quantified their possible occurrence and variability in frequency and resonance location for the first time. We find that cFMRs are supported most often in the dawn sector compared to dusk and noon, since the large densities associated with the plasmaspheric plume or an extended plasmasphere in these sectors can preclude cFMR occurence. This possible occurrence in our calculations is consistent with the occurrence of observed discrete field line resonances (FLRs) on the ground [*Baker et al.*, 2003; *Plaschke et al.*, 2008], though numerous other mechanisms for their excitation also exist. The computed eigenfrequencies are within the range of previously observed [*Baker et al.*, 2003; *Plaschke et al.*, 2008; *Hartinger et al.*, 2013] and theoretical results [*Mann et al.*, 1999; *Claudepierre et al.*, 2009], at typically a few mHz around dawn/dusk and tens of mHz at noon. The variability, however, is found to be much larger in the noon and dusk sectors, chiefly due to the density, whereas magnetic field changes have a comparable contribution around dawn. Overall the relative spread (ratio of median absolute deviation to the median) is estimated to be 28%, 72% and 55% at dawn, noon and dusk respectively. Finally, the observed bimodal distribution in outer-magnetospheric density at dawn results in bimodal cFMR frequency distributions, whereby the secondary population have the low "CMS" frequencies often attributed to FMRs [*Samson et al.*, 1992] that have been called into question by some [*Harrold and Samson*, 1992; *Allan and McDiarmid*, 1993].

Future work should validate the calculated frequencies and resonance locations against observations both in space and on the ground, taking particular care in unambiguously identifying the ULF mode and driver where possible. Furthermore, by parameterising the collated density profiles in this study it should be possible to ascertain the dependence of cFMR occurrence and frequencies on e.g. the plasmapause position or radial density exponent [*Allan and McDiarmid*, 1989; *Wright and Rickard*, 1995] and with solar wind and magnetospheric conditions e.g. P_{dyn} or Kp. This would allow the prediction of FMR frequencies and the discrete standing Alfvén waves they excite, of interest to e.g. the radiation belt community [*Elkington*, 2006].

Acknowledgments. MOA thanks A. N. Wright and Y. Nishimura for helpful discussions. We acknowledge NASA contract NAS5-02099 and the THEMIS Mission, specifically J. W. Bonnell and F. S. Mozer for EFI data and C. W. Carlson and J. P. McFadden for ESA data. The OMNI data was obtained from the NASA/GSFC OMNIWeb interface at http://omniweb.gsfc.nasa.gov.

References

Allan, W., and D. R. McDiarmid, Magnetospheric cavity modes and field-line resonances: the effect of radial mass density variation, *Planet. Space Sci.*, *37*, 407–418, doi:10.1016/0032-0633(89)90122-0, 1989.

Allan, W., and D. R. McDiarmid, Frequency ratios and resonance positions for magnetospheric cavity/waveguide modes, *Ann. Geophys.*, *11*, 916–924, 1993.

Angelopoulos, V., The THEMIS mission, *Space Sci. Rev.*, *141*, 5–34, doi:10.1007/s11214-008-9336-1, 2008.

Archer, M. O., and F. Plaschke, What frequencies of standing surface waves can the subsolar magnetopause support?, *J. Geophys Res.*, *120*, 3632–3646, doi: 10.1002/2014JA020545, 2015.

Archer, M. O., T. S. Horbury, J. P. Eastwood, J. M. Weygand, and T. K. Yeoman, Magnetospheric response to magnetosheath pressure pulses: A low pass filter effect, *J. Geophys. Res.*, *118*, 5454–5466, doi:10.1002/jgra.50519, 2013a.

Archer, M. O., M. D. Hartinger, and T. S. Horbury, Magnetospheric "magic" frequencies as magnetopause surface eigenmodes, *Geophys. Res. Lett.*, *40*, 5003–5008, doi: 10.1002/grl.50979, 2013b.

Baker, G. J., E. F. Donovan, and B. J. Jackel, A comprehensive survey of auroral latitude Pc5 pulsation characteristics, *J. Geophys. Res.*, *108*, SMP 11–1, doi: 10.1029/2002JA009801, 2003.

Bonnell, J. W., F. S. Mozer, G. T. Delory, A. J. Hull, R. E. Ergun, C. M. Cully, V. Angelopoulos, and P. R. Harvey, The electric field instrument (EFI) for THEMIS, *Space Sci. Rev.*, *141*, 303–341, doi:10.1007/s11214-008-9469-2, 2008.

Bowman, A. W., and A. Azzalini, *Applied Smoothing Techniques for Data Analysis*, Oxford University Press, 1997.

Carpenter, D. L., and R. R. Anderson, An ISEE/whistler model of equatorial electron density in the magnetosphere, *J. Geophys Res.*, *97*, 1097–1108, doi:10.1029/91JA01548, 1992.

Chen, L., and A. Hasegawa, A theory of long-period magnetic pulsations: 1. steady state excitation of field line resonance, *J. Geophys Res.*, *79*, 1024–1032, doi: 10.1029/JA079i007p01024, 1974.

Chisham, G., and D. Orr, A statistical study of the local time asymmetry of Pc5 ULF wave characteristics observed at midlatitudes by SAMNET, *J. Geophys. Res.*, *102*, 24,339–24,350, doi:10.1029/97JA01801, 1997.

Claudepierre, S. G., M. Wiltberger, S. R. Elkington, W. Lotko, and M. K. Hudson, Magnetospheric cavity modes driven by solar wind dynamic pressue fluctuations, *Geophys.*

Res. Lett., *36*, L13,101, doi:10.1029/2009GL039045, 2009.

Claudepierre, S. G., M. K. Hudson, W. J. G. Lotko, W.Lotko, and R. E. Denton, Solar wind driving of magnetospheric ULF waves: Field line resonances driven by dynamic pressure fluctuations, *J. Geophys Res.*, *115*, A11,202, doi:10.1029/2010JA015399, 2010.

Darrouzet, F., J. de Keyser, Décréau, F. El Lemdani-Mazouz, and X. Valliéres, Statistical analysis of plasmaspheric plumes with Cluster/WHISPER observations, *Ann. Geophys.*, *26*, 2403–2417, doi:10.5194/angeo-26-2403-2008, 2008.

Denton, R. E., K. Takahashi, J. Lee, C. K. Zeitler, N. T. Wimer, L. E. Litscher, H. J. Singer, and K. Min, Field line distribution of mass density at geostationary orbit, *J. Geophys Res.*, *120*, 4409–4422, doi:10.1002/2014JA020810, 2015.

Elkington, S. R., A review of ULF interactions with radiation belt electrons, in *Magnetospheric ULF Waves: Synthesis and New Directions*, *Geophysical Monograph Series*, vol. 169, edited by K. Takahashi, P. J. Chi, R. E. Denton, and R. L. Lysak, John Wiley & Sons, doi:10.1029/169GM06, 2006.

Fenrich, F. M., J. C. Samson, G. Sofko, and R. A. Greenwald, ULF high- and low-m field line resonances observed with the Super Dual Auroral Radar Network, *J. Geophys. Res.*, *100*, 21,535–21,547, doi:10.1029/95JA02024, 1995.

Harrold, B. G., and J. C. Samson, Standing ulf modes of the magnetosphere: A theory, *Geophys. Res. Lett.*, *19*, 1811–1814, doi:10.1029/92GL01802, 1992.

Hartinger, M. D., V. Angelopoulos, M. B. Moldwin, Y. Nishimura, D. L. Turner, K.-H. Glassmeier, M. G. Kivelson, J. Matzka, and C. Stolle, Observations of a Pc5 global (cavity/waveguide) mode outside the plasmasphere by THEMIS, *J. Geophys. Res.*, *117*, A06,202, doi:10.1029/2011JA017266, 2012.

Hartinger, M. D., V. Angelopoulos, M. B. Moldwin, K. Takahashi, and L. B. N. Clausen, Statistical study of global modes outside the plasmasphere, *J. Geophys. Res.*, *118*, 804–822, doi:10.1002/jgra.50140, 2013.

Hartinger, M. D., D. Welling, N. M. Viall, M. B. Moldwin, and A. Ridley, The effect of magnetopause motion on fast mode resonance, *J. Geophys Res.*, *119*, 8212–8227, doi:10.1002/2014JA020401, 2014.

Hartinger, M. D., M. B. Moldwin, S. Zou, J. W. Bonnell, and V. Angelopoulos, ULF wave electromagnetic energy flux into the ionosphere: Joule heating implications, *J. Geophys Res.*, *120*, 494–510, doi:10.1002/2014JA020129, 2015.

Huber, P. J., *Robust Statistics*, Wiley Series in Probability, John Wiley & Sons, 1981.

Kabin, K., R. Rankin, C. L. Waters, R. Marchand, E. F. Donovan, and J. C. Samson, Different eigenproblem models for field line resonances in cold plasma: Effect on magnetospheric density estimates, *Planet. Space Sci.*, *55*, 820–828, doi:10.1016/j.pss.2006.03.014, 2007.

Khazanov, G. V., *Kinetic Theory of the Inner Magnetospheric Plasma*, chap. Analysis of Cold Plasma Transport, pp. 193–269, Astrophysics and Space Science Library, Springer, 2011.

Kivelson, M. G., and D. J. Southwood, Resonant ULF waves: a new interpretation, *Geophys. Res. Lett.*, *12*, 49–52, doi:10.1029/GL012i001p00049, 1985.

Kivelson., M. G., J. Etcheto, and J. G. Trotignon, Global compressional oscillations of the terrestrial magnetosphere: The evidence and a model, *J. Geophys Res.*, *89*, 9851–9856, doi:10.1029/JA089iA11p09851, 1984.

Kokubun, S., ULF waves in the outer magnetosphere: Geotail observation 1 transverse waves, *Earth Planets Space*, *65*, 411–433, doi:10.5047/eps.2012.12.013, 2013.

Lee, J. H., and V. Angelopoulos, On the presence and properties of cold ions near earth's equatorial magnetosphere, *J. Geophys Res.*, *119*, 1749–1770, doi:10.1002/2013JA019305, 2014.

Liu, X., and W. Liu, A new plasmplasma location model based on THEMIS observations, *Sci. China Earth Sci.*, *57*, 2252–2557, doi:10.1007/s11430-014-4844-1, 2014.

Mann, I. R., A. N. Wright, K. J. Mills, and V. M. Nakariakov, Excitation of magnetospheric waveguide modes by magnetosheath flows, *J. Geophys Res.*, *104*, 333–353, doi:10.1029/1998JA900026, 1999.

Mann, I. R., et al., Discovery of the action of a geophysical synchrotron in the Earth's Van Allen radiation belts, *Nature Commun.*, *4*, 2795, doi:10.1038/ncomms3795, 2013.

Mathie, R. A., I. R. Mann, F. W. Menk, and D. Orr, Pc5 ULF pulsations associated with waveguide modes observed with the IMAGE magnetometer array, *J. Geophys. Res.*, *104*, 7025–7036, doi:10.1029/1998JA900150, 1999.

McFadden, J. P., C. W. Carlson, D. Larson, M. Ludlam, R. Abiad, B. Elliott, P. Turin, M. Marckwordt, and V. Angelopoulos, The THEMIS ESA plasma instrument and in-flight calibration, *Space Sci. Rev.*, *141*, 277–302, doi:10.1007/s11214-008-9440-2, 2008a.

McFadden, J. P., C. W. Carlson, J. Bonnell, F. Mozer, V. Angelopoulos, K. H. Glassmeier, and U. Auster, THEMIS ESA first science results and performance issues, *Space Sci. Rev.*, *141*, 447–508, doi:10.1007/s11214-008-9433-1, 2008b.

Moore, T. E., D. L. Gallagher, J. L. Horwitz, and R. H. Comfort, MHD wave breaking in the outer plasmasphere, *Geophys. Res. Lett.*, *14*, 1007–1010, doi: 10.1029/GL014i010p01007, 1987.

O'Brien, T. P., and M. B. Moldwin, Empirical plasmapause models from magnetic indices, *Geophys. Res. Lett.*, *30*, 1152, doi:10.1029/2002GL016007, 2003.

Plaschke, F., K. H. Glassmeier, O. D. Constantinescu, I. R. Mann, D. K. Milling, U. Motschmann, and I. J. Rae, Statistical analysis of ground based magnetic field measurements with the field line resonance detector, *Ann. Geophys.*, *26*, 3477–3489, doi:10.5194/angeo-26-3477-2008, 2008.

Radoski, H. R., A note on the problem of hydromagnetic resonances in the magnetosphere, *Planet. Space Sci.*, *19*, 1012–1013, doi:10.1016/0032-0633(71)90152-8, 1971.

Rankin, R., K. Kabin, and R. Marchand, Alfvénic field line resonances in arbitrary magnetic field topology, *Adv. Space Res.*, *38*, 1720–1729, doi:10.1016/j.asr.2005.09.034, 2006.

Rickard, G. J., and A. N. Wright, Alfvén resonance excitation and fast wave propagation in magnetospheric waveguides, *J. Geophys. Res.*, *99*, 13,455–13,464, doi: 10.1029/94JA00674, 1994.

Rickard, G. J., and A. N. Wright, ULF pulsations in a magnetospheric waveguide: Comparison of real and simulated satellite data, *J. Geophys. Res.*, *100*, 3,531–3,537, doi: 10.1029/94JA02935, 1995.

Samson, J. C., R. A. Greenwald, J. M. Ruohoniemi, T. J. Hughes, and D. D. Wallis, Magnetometer and radar observations of magnetohydrodynamic cavity modes in the Earth's magnetosphere, *Can. J. Phys.*, *69*, 929–937, doi:10.1139/p91-147, 1991.

Samson, J. C., B. G. Harrold, J. M. Ruohoniemi, R. A. Greenwald, and A. D. M. Walker, Field line resonances associated with MHD waveguides in the magnetosphere, *Geophys. Res. Lett.*, *19*, 441–444, doi:10.1029/92GL00116, 1992.

Samson, J. C., C. L. Waters, F. W. Menk, and B. J. Fraser, Fine structure in the spectra of low latitude field line resonances, *Geophys. Res. Lett.*, *22*, 2111–2114, doi:10.1029/95GL01770, 1995.

Sarris, T. E., W. Liu, X. Li, K. Kabin, E. R. Talaat, R. Rankin, V. Angelopoulos, J. Bonnell, and K. H. Glassmeier, THEMIS observations of the spatial extent and pressure-pulse excitation of field line resonances, *Geophys. Res. Lett.*, *37*, L15,104, doi:10.1029/2010GL044125, 2010.

Sheeley, B. W., M. B. M. B. Moldwin, H. K. Rassoul, and R. R. Anderson, An empirical plasmasphere and trough density model: CRRES observations, *J. Geophys Res.*, *106*, 25,631–25,641, doi:10.1029/2000JA000286, 2001.

Singer, H. J., D. J. Southwood, R. J. Walker, and M. G. Kivelson, Alfvén wave resonances in a realistic magnetospheric magnetic field geometry, *J. Geophys. Res.*, *86*, 4589–4596, doi:10.1029/JA086iA06p04589, 1981.

Smit, G. R., Oscillatory motion of the nose region of the magnetopause, *J. Geophys. Res.*, *73*, 4990–4993, doi:10.1029/JA073i015p04990, 1968.

Southwood, D. J., Some features of field line resonances in the magnetosphere, *Planet. Space Sci.*, *22*, 483–491, doi:10.1016/0032-0633(74)90078-6, 1974.

Stephenson, J. A., and A. D. M. Walker, HF radar observations of Pc5 ULF pulsations driven by the solar wind, *Geophys. Res. Lett.*, *29*, 8–1 – 8–4, doi:10.1029/2001GL014291, 2002.

Takahashi, K., R. E. Denton, and H. J. Singer, Solar cycle variation of geosynchronous plasma mass density derived from the frequency of standing alfvén waves, *J. Geophys Res.*, *115*, A07,207, doi:10.1029/2009JA015243, 2010.

Takahashi, K., R. E. Denton, M. Hirahara, K. Min, S. Ohtani, and E. Sanchez, Solar cycle variation of plasma mass density in the outer magnetosphere: Magnetoseismic analysis of toroidal standing Alfvén waves detected by Geotail, *J. Geophys. Res.*, *119*, 8338–8356, doi:10.1002/2014JA020274, 2014.

Tsyganenko, N. A., Modeling the earth's magnetospheric magnetic field confined within a realistic magnetopause, *J. Geophys. Res.*, *100*, 5599–5612, doi:10.1029/94JA03193, 1995.

Tsyganenko, N. A., Effects of the solar wind conditions in the global magnetospheric configurations as deduced from data-based field models, in *International Conference on Substorms, Proceedings of the 3rd International Conference held in Versailles*, edited by E. Rolfe and B. Kaldeich, p. 181, European Space Agency, Paris, 1996.

Tu, J., P. Song, B. W. Reinisch, and J. L. Green, Smooth electron density transition from plasmasphere to the subauroral region, *J. Geophys. Res.*, *112*, A05,227, doi: 10.1029/2007JA012298, 2007.

Viall, N. M., L. Kepko, and H. E. Spence, Relative occurrence rates and connection of discrete frequency oscillations in the solar wind density and dayside magnetosphere, *J. Geophys. Res.*, *114*, A01,201, doi:10.1029/2008JA013334, 2009.

Walker, A. D. M., J. M. Ruohoniemi, K. B. Baker, R. A. Greenwald, and J. C. Samson, Spatial and temporal behavior of ULF pulsations observed by the Goose Bay HF radar, *J. Geophys. Res.*, *97*, 12,187–12,202, doi:10.1029/92JA00329, 1992.

Walsh, B. M., D. G. Sibeck, Y. Nishimura, and V. Angelopoulos, Statistical analysis of the plasmaspheric plume at the magnetopause, *J. Geophys Res.*, *118*, 4844–4851, doi:10.1002/jgra.50458, 2013.

Waters, C. L., B. G. Harrold, F. W. Menk, J. C. Samson, and B. J. Fraser, Field line resonances and waveguide modes at low latitudes 2. a model, *J. Geophys Res.*, *105*, 7763–7774, doi:10.1029/1999JA900267, 2000.

Waters, C. L., K. Takahashi, D.-H. Lee, and B. J. Anderson, Detection of ultralow-frequency cavity modes using spacecraft data, *J. Geophys. Res*, *107*, 1284, doi: 10.1029/2001JA000224, 2002.

Wild, J. A., T. K. Yeoman, and C. L. Waters, Revised time of flight calculations for high latitude geomagnetic pulsations using a realistic magnetospheric magnetic field model, *J. Geophys. Res.*, *110*, A11,206, doi:10.1029/2004JA010964, 2005.

Wright, A. N., Dispersion and wave coupling in inhomogeneous MHD waveguides, *J. Geophys. Res.*, *99*, 159–167, doi:10.1029/93JA02206, 1994.

Wright, A. N., and G. J. Rickard, ULF pulsations driven by magnetopause motions: Azimuthal phase characteristics, *J. Geophys. Res.*, *100*, 23,703–23,710, doi: 10.1029/95JA01765, 1995.

Ziesolleck, C. W. S., and D. R. McDiarmid, Statistical survey of auroral latitude Pc5 spectral and polarization characteristics, *J. Geophys. Res.*, *100*, 19,299–19,312, doi:

10.1029/95JA00434, 1995.

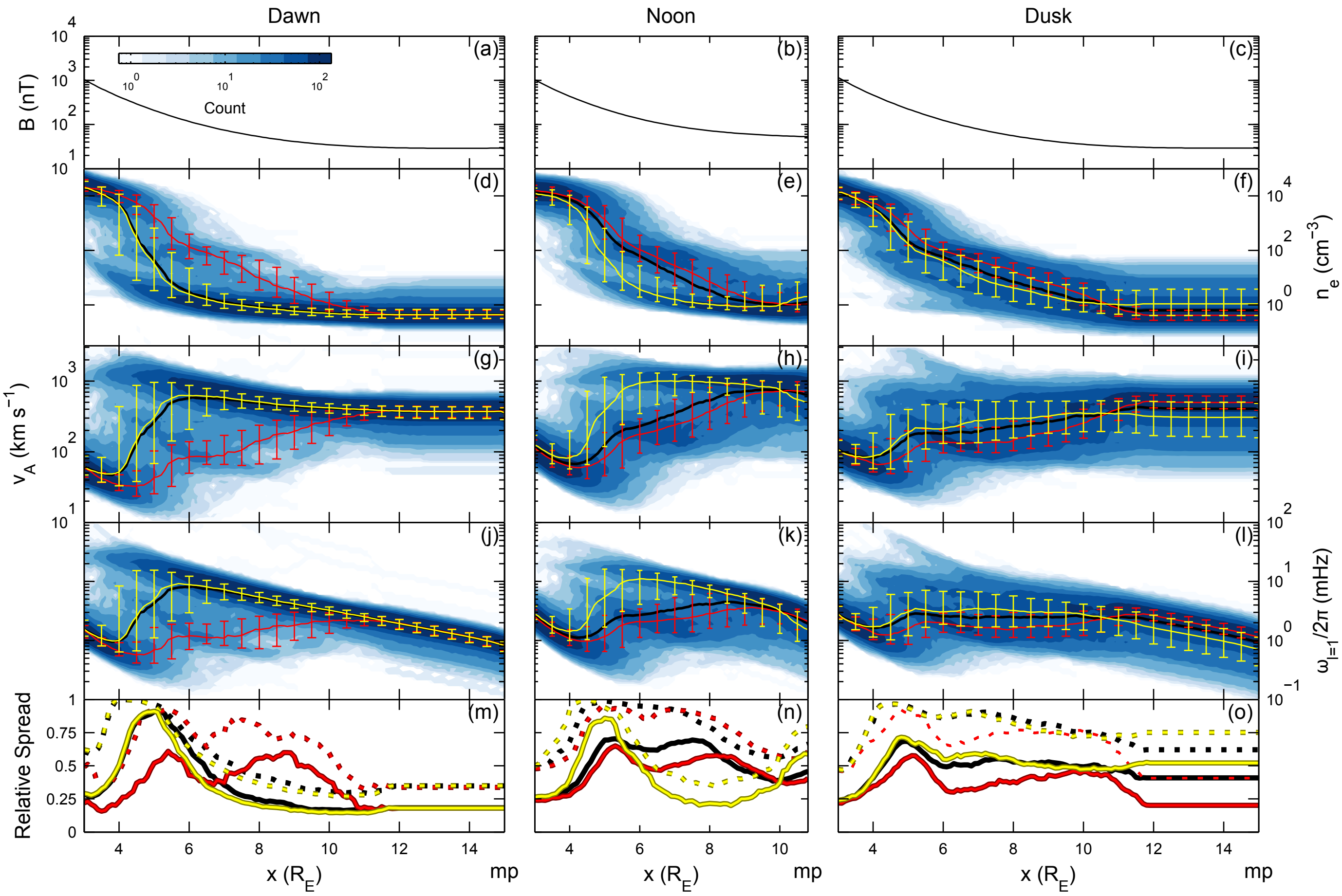

Figure 1: Profiles as a function of radial distance in the dawn (left), noon (middle) and dusk (right) sectors of equatorial (a–c) magnetic field strength, (d–f) electron number density, (g–i) Alfvén speed, (j–l) fundamental FLR frequency, (m–o) relative spreads in the density (dotted) and speed/frequency (solid). Medians (solid lines) and interquartile ranges (error bars) are shown over all profiles (black), profiles which support a fundamental cFMR (yellow), and profiles which don't (red).

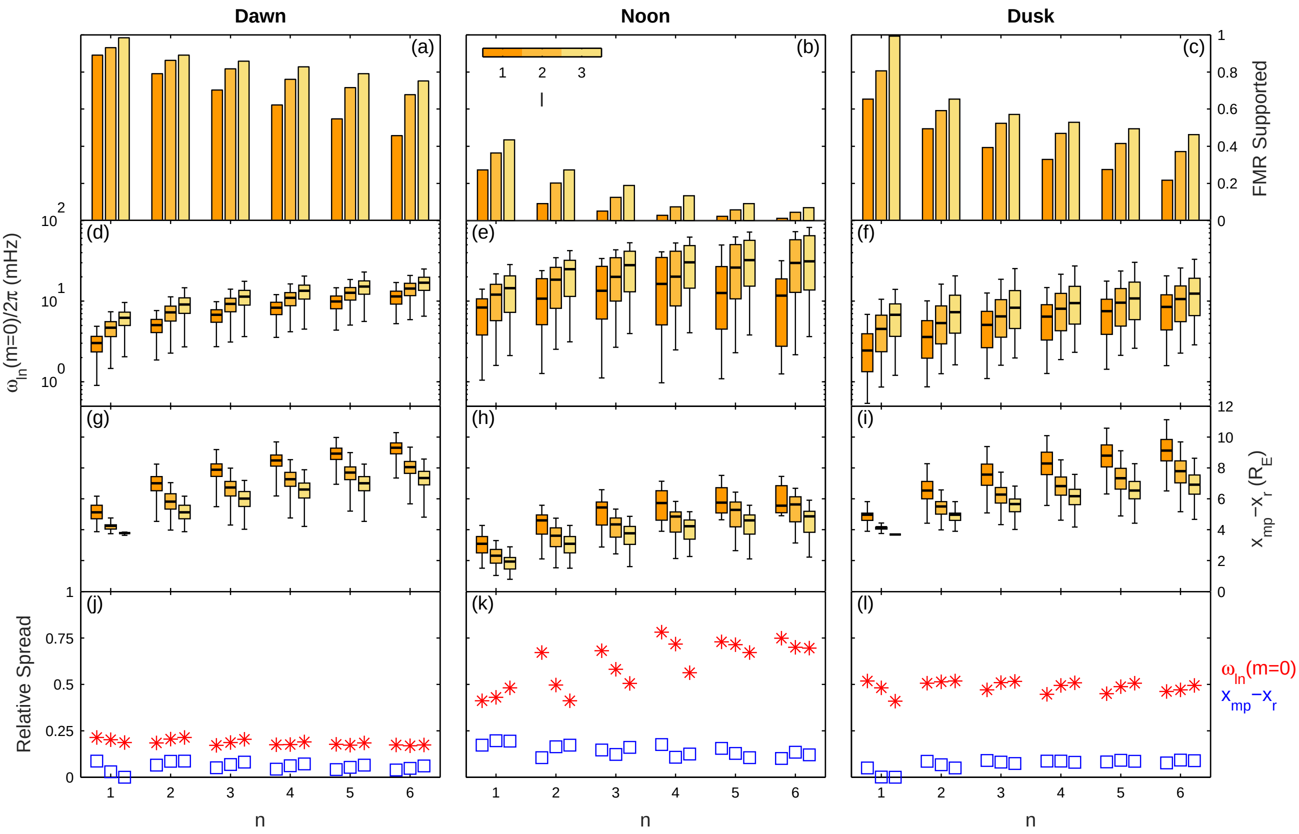

Figure 2: cFMR results as a function of n (groups) and l (colours) for $m = 0$ in the dawn (left), noon (middle) and dusk (right) sectors. (a–c) Fraction of cFMRs supported, (d–f) cFMR frequency and (g–i) cavity size as box plots with whiskers indicating 95% of the data, (j–l) relative spreads in the frequency (red) and cavity size (blue).

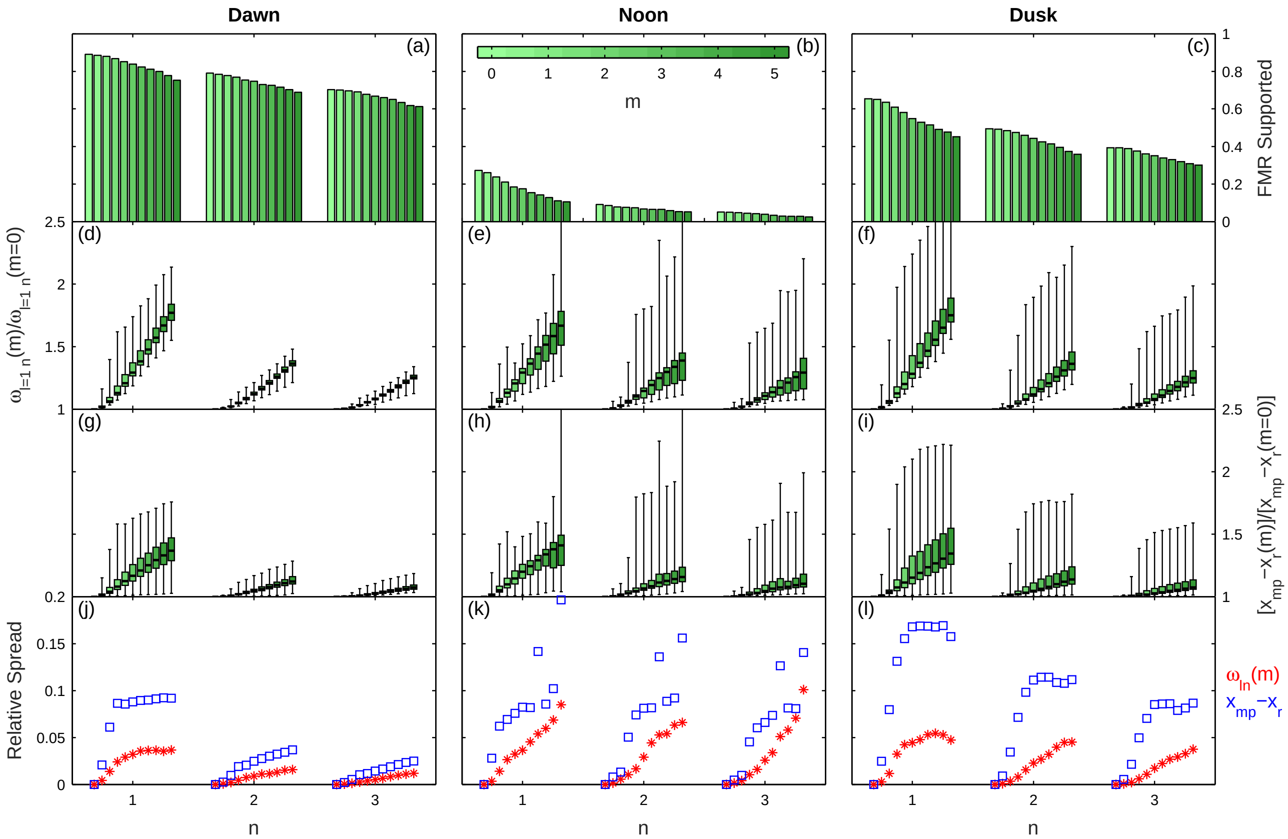

Figure 3: cFMR results as a function of n and m for $l = 1$ in a similar format to Figure 2. In panels d–l ratios to the $m = 0$ results are shown.

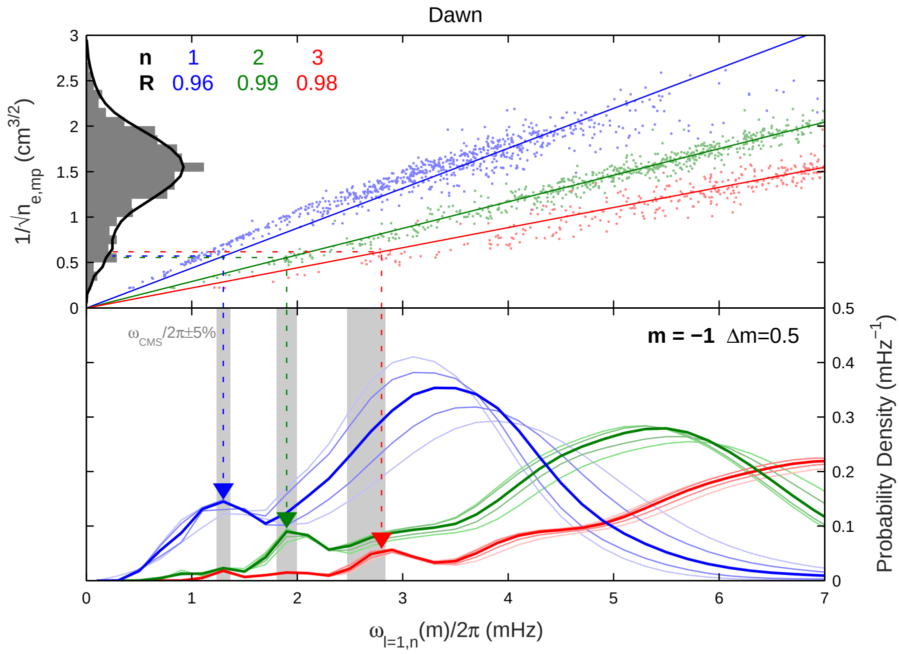

Figure 4: (Top) Relationship between cFMR frequency ($n = 1$–3 in blue, green, red) and the reciprocal square root of the outer-magnetospheric density (at apogee) at dawn. A histogram (grey) and kernel density estimate (KDE, black) of the latter is also shown. (Bottom) KDEs of the cFMR frequency distributions. Shaded areas show the CMS frequencies ±5%.